JOURNAL OF AIRCRAFT
Vol. 48, No. 3, May–June 2011

Flight Mechanical Evaluation of Approaches

Monique Heiligers,* Theo van Holten,* and Max Mulder*
Delft University of Technology, 2629 HS Delft, The Netherlands

DOI: 10.2514/1.C031187

The task demand load experienced by a pilot while flying an approach is influenced by, among others, the following two factors: first, whether it is possible to meet the altitude and airspeed constraints defined at the waypoints, and second, whether it is possible to achieve a stabilized approach at 1000 ft. To be able to analyze an approach with respect to these two factors, a flight mechanical assessment tool based on a Monte Carlo simulation is presented in this paper. The Monte Carlo simulation predicts (given the aircraft, the standard operating procedures, the wind conditions, and the approach trajectory) the percentage of flights that will not meet the constraints at the waypoints and will not achieve a stabilized approach. The Monte Carlo simulation can be used by approach designers, as it will provide insight into the flight mechanical feasibility of an approach as well as give an indication of the task demand load that will be experienced by pilots. To demonstrate the results of the Monte Carlo simulation, a fictitious approach is considered in a case study.

I. Introduction

APPROACH- and landing-phase accidents account for a significant proportion of air transport accidents. The Flight Safety Foundation Approach-and-Landing Accident Reduction (ALAR) Task Force [1] has performed comprehensive research with respect to approach and landing accident reduction. Approximately 59% of the world jet-fleet accidents to date occurred in these flight phases and accounted for 29% of all fatalities [2]. The most frequent causal factors are related to crew performance, emphasizing the need to better understand which factors complicate an approach for a flight crew and which factors in an approach increase the chance of accidents.

In addition, a considerable growth in the air transport industry is expected, with forecasts indicating that air traffic movements around the world will increase significantly [3]. This growth is likely to cause extra congestion and delays, which in turn calls for upgrading the overall system capacity. Part of the capacity increase could come from the design of new approach trajectories, possibly including curved approaches, the use of higher approach altitudes, continuous descent approaches, etc. Before these new approaches can be introduced, it is mandatory to investigate whether these approaches are more complicated for a pilot to fly.

The overall goal of the research presented in this paper and its companion [4] is to develop a method that can predict how complicated an approach will be for a pilot. That is, our research should be able to provide an accurate prediction of what we call the pilot task demand load (TDL) for any (existing or to be designed) approach. Note that TDL is defined as the mental workload imposed by the system to be controlled or supervised [5], and it is not to be mistaken for the mental workload as experienced by the human operator, which is referred to as mental load (ML). Whereas the latter measure depends on, for instance, individual operator training, motivation, and mental capacities, the TDL attempts to capture the external demand and the effort needed to reach the goals defined.

Overall, our hypothesis is that the task demand during an approach is mainly affected by the external constraints put on the pilot/aircraft system. In the accompanying paper [4], it is experimentally demonstrated that pilot mental workload (as reported subjectively by professional airline pilots) is influenced by localizer-intercept speed, localizer-intercept angle, the lineup distance (distance between runway threshold and intermediate fix), the altitude of the final approach fix (FAF), whether the altitude and velocity constraints at the waypoints (WPs) can be met, and whether a stabilized approach at 1000 ft can be achieved. Clearly, then, these external constraints form (some of) the systematic elements that (together) make an approach more difficult to perform, or not. In other words, these are the factors that determine the external demand and, therefore, the pilot TDL.

The accompanying paper [4] thus shows that pilot ML increases significantly when the aircraft is unable to meet the altitude and velocity constraints at the WPs, and when a stabilized approach at 1000 ft cannot be achieved. This paper presents a flight mechanical assessment tool that allows the approach designer to study in advance the effects of these two factors. It predicts the percentage of flights where aircraft are unable to, first, meet the constraints at the WPs and, second, will not achieve a stabilized approach. The tool allows the approach designer to freely vary aircraft characteristics (e.g., weight), the wind conditions, the approach trajectory, the constraints at the WPs, and the standard operating procedures (SOPs). Apart from the fact that this information is useful for the flight mechanical design of the approach, it will also give the approach designer an indication of pilot TDL.

The paper starts with an explanation of the basic principles and assumptions for the method to predict pilot TDL. Next, the Monte Carlo computer simulation that forms the flight mechanical assessment tool is explained in detail. Since the Monte Carlo computer simulation is quite elaborate, and requires some time to run, a point mass model (PMM) for initial estimates (regarding the possibility of meeting the constraints at the WPs and achieving a stabilized approach) is subsequently presented. Then, in order to demonstrate the output and predictions of the flight mechanical assessment tool, a case study is presented, followed by the conclusions and recommendations.

II. Basic Principles of Method to Predict Pilot Task Demand Load

This section explains the basic principles of the method to predict pilot TDL; that is, the assumptions and the choices that have been made as to what is incorporated within this research, and what is currently considered to be beyond the scope of this research. As explained before, the flight mechanical assessment tool is linked to the research on pilot TDL and is therefore based on the same assumptions.

A. Factors of Air Transport System Included

Many different factors and the interactions between those factors have an influence on the execution of an approach; see Fig. 1. The

Received 23 July 2010; revision received 27 October 2010; accepted for publication 28 October 2010.

*Faculty of Aerospace Engineering.

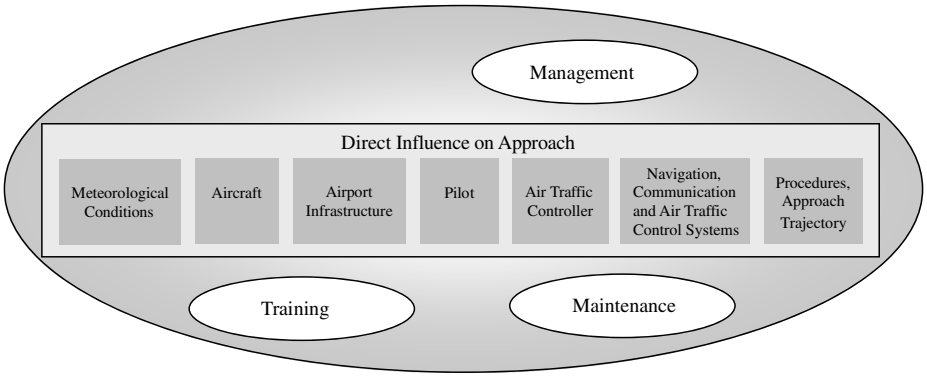

Fig. 1 Direct and indirect factors that influence the safety of airport approaches.

research on pilot TDL obviously concentrates on the pilot box in Fig. 1. To determine pilot TDL, this research will only take into account the factors that have a direct influence on an approach (see Fig. 1): most important, the characteristics of the trajectory, the type of aircraft, and the meteorological conditions.

B. Approaches Considered and Automation Used

Obviously, pilot TDL directly depends on the type of approach that is considered. This research focuses on area navigation (RNAV) approaches. Although it is appreciated that nonprecision approaches, such as nondirectional beacon approaches, are in general more difficult for a pilot to fly than RNAV approaches [6], a deliberate choice is made to focus on RNAV approaches, since these are expected to become more and more frequently used in the future. The last part of the RNAV approach is assumed to be flown using the instrument landing system (ILS).

The part of the flight that is considered in the method to predict pilot TDL and in the flight mechanical assessment tool starts at the initial approach fix (IAF) and comprises the entire approach (initial approach, intermediate approach, and final approach) until 1000 ft above airport elevation; see Fig. 2. Based on interviews with pilots, it was decided to use two different levels of automation during the approach: until localizer-intercept heading, the approach is flown using the flight management system (FMS), autopilots, and autothrottle. At localizer-intercept heading (but before localizer capture), the pilot switches to flight director (FD) mode and disconnects the autothrottle; the remainder of the approach is thus flown using the FMS and FD, which implies manual control by the pilot.

C. Nonnominal Conditions and Emergencies

Nonnominal conditions and emergencies, such as engine failure, are not considered in this research. The goal is to determine pilot TDL for published RNAV approaches under nominal conditions. When any emergencies such as engine failure occur, the crew will most likely not be required to follow the RNAV approach anyway, but they will be vectored to the runway in the most convenient way.

Additionally, the assumption for less severe nonnominal situations is that, when flying under nominal conditions, the RNAV approach should provide enough margin with respect to pilot TDL such that the pilot has enough spare capacity and time to deal with nonnominal conditions. This implies that the TDL that is predicted by this research for nominal conditions should be well below the absolute maximum TDL a pilot can cope with in order to guarantee this margin. Therefore, the simulation of nonnominal conditions is not part of the flight mechanical assessment tool.

D. Boundary Conditions: Stabilized Approach and Standard Operating Procedures

The TDL experienced by the pilot also depends on the boundary conditions that are set, e.g., the accuracy with which the approach needs to be flown. The boundary conditions chosen for this research and for the flight mechanical assessment tool are that the approach should be performed according to SOPs and that pilots should aim to achieve a stabilized approach at 1000 ft above airport elevation. This decision is based on the conclusions of the ALAR Task Force [1] that stated, "Establishing and adhering to adequate SOPs and flight-crew decision making processes improve approach-and-landing safety," and, "Unstabilized and rushed approaches contribute to approach-and-landing accidents."

To determine whether a stabilized approach is achieved at 1000 ft, the following nine criteria are used [1]:

1) The aircraft is on the correct flight path.

2) Only small changes in heading/pitch are required to maintain the correct flight path.

3) The aircraft speed is not more than the reference speed (VREF) plus 20 kt indicated airspeed (IAS), and it is not less than the VREF.[†]

4) The aircraft is in the correct landing configuration.

5) Sink rate is no greater than 1000 ft per minute; if an approach requires a sink rate greater than 1000 ft per minute, a special briefing should be conducted.

6) The power setting is appropriate for the aircraft configuration and is not below the minimum power for approach as defined by the aircraft operating manual.

7) All briefings and checklists have been conducted.

8) Specific types of approaches are stabilized if they also fulfill the following: ILS approaches must be flown within one dot[‡] of glide slope and localizer; a category II or category III ILS approach must be flown within the expanded localizer band; and during a circling approach, wings should be level on final when the aircraft reaches 300 ft above airport elevation.

9) Unique approach procedures or abnormal conditions requiring a deviation from the preceding elements of a stabilized approach require a special briefing.

E. Level of Detail of Computer Simulation Models

The approach we have chosen to predict pilot TDL [7] deviates from the philosophy behind human operator models, such as the procedure-oriented crew model [8,9] or the man–machine integrated design and analysis system [10–12]. Our approach to predict pilot TDL is based on the principles of cognitive work analysis [13]. The main characteristic of cognitive work analysis is that it shifts the emphasis from investigating the constraints of the human operator (like memory capacity, time delay, etc.) to analyzing and describing operator environment (like the trajectory, the aircraft dynamics, the wind conditions, etc.). The reason for this choice is that the constraints in the environment actually shape the behavior of the human working in that environment. By choosing the approach to focus on operator environment instead of the human operator, the model will be more accessible and easier to use for approach designers, who often have little background in human operator modeling (or none).

Therefore, the goal is to incorporate detailed models of the environment of the pilot in the flight mechanical assessment tool and to add to this a rather simple model for the pilot. Consequently, the

[†]VREF is defined as 1.3 times the stall speed.

[‡]One dot deviation on glide slope equals 0.7° beam error, and one dot deviation on the localizer equals 2.5° beam error.

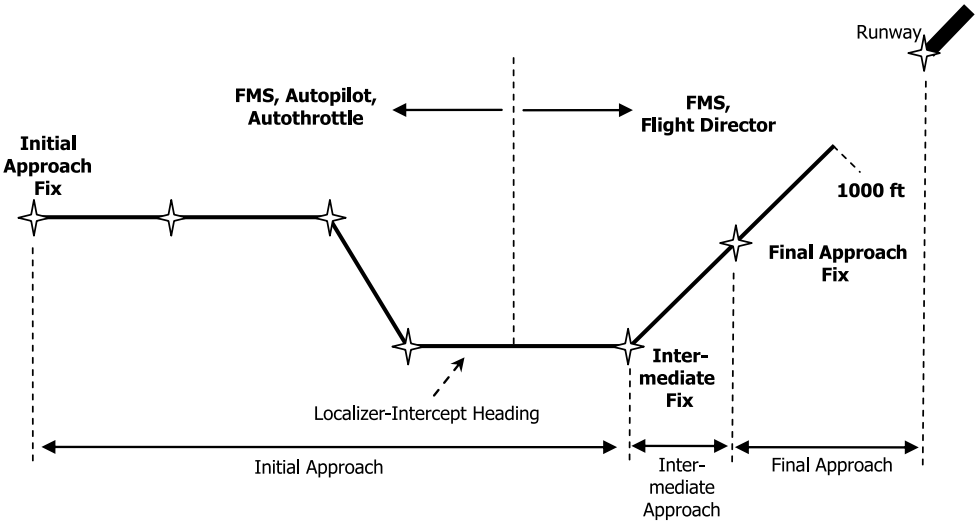

Fig. 2 Part of flight considered (top view) and automation used.

aircraft with its kinematic and dynamic constraints (the three-dimensional properties of the trajectory, the velocity profile, turbulence, wind, etc.), in other words, the factors that have a direct influence on an approach as given in Fig. 1, are modeled in as much detail and accuracy as possible. The pilot model consists of a continuous manual control model (which, in effect, only contains a pure gain plus time delay) and a model for performing discrete actions, such as selecting flaps and gear, according to the SOPs.

III. Monte Carlo Computer Simulation

The flight mechanical assessment tool consists of a Monte Carlo computer simulation based on the basic principles and assumptions, as explained in the previous section. When a newly designed approach is entered into the computer simulation, the simulation predicts whether the constraints at the WPs will be met and whether a stabilized approach can be achieved at 1000 ft. It also predicts under what circumstances (e.g., wind conditions) this can be achieved. This section will describe the aircraft model, pilot model, SOPs, wind model, and turbulence model that are used within the Monte Carlo computer simulation.

A. Computer Simulation Input

The input of the Monte Carlo computer simulation consists of a list of WPs defined by their latitude–longitude coordinates and the altitude and speed constraints at these WPs. At the moment, the only constraints that can be handled by the simulation are at constraints, meaning that at a certain WP, the aircraft should be at a certain altitude and at a certain speed (at or above constraints are not yet possible). Additionally, the user has to define which WP in the list is the FAF.

B. Aircraft (Boeing 747-100), Autopilot, and Flight Director Models

Although the Monte Carlo simulation should eventually work for any aircraft type, for now, a Boeing 747 (B747) aircraft model is used in the simulation. The nonlinear aircraft model is based on the B747-100 documentation by Hanke and Nordwall [14] and is modeled in as much detail as possible. Autopilot, autothrottle, and FD models are also derived from [14]. Autopilot modes included are lateral navigation (LNAV), altitude hold, altitude select, glide slope, vertical navigation (VNAV), heading select, and localizer modes. The LNAV mode is based on the very high-frequency omnidirectional range modes described in [14], and the VNAV mode is based on the vertical speed mode described in [14], where the selected (calculated) vertical speed depends on the constraints at the WPs and the wind conditions.

The hierarchy in meeting the constraints at the WPs is as follows. The autopilot and FD modes will always aim to meet the altitude constraints at the WPs. Second to this, the autothrottle controls the airspeed. This results in the situation that the altitude constraint at the

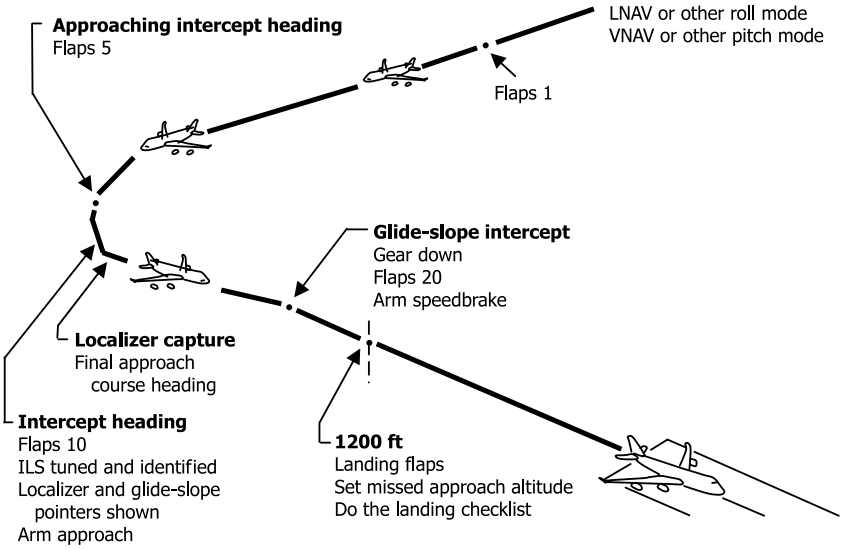

Fig. 3 SOPs for B747 delayed flap approach.

Table 1 Trigger events and reaction time distributions for pilot actions in Monte Carlo simulation

Pilot action	Trigger Event	Mean	Standard deviation
Flaps 1	Reaching first WP of leg on which aircraft is 20 nm from field	$T/3$ [a]	$T/3$ [a]
Flaps 5	Reaching first WP of leg-before-localizer-intercept heading	$2 \cdot T/3$ [b]	$T/3$ [b]
Autothrottle/autopilot off	Turn to localizer-intercept heading	$T/2$ [c]	$T/2$ [c]
Flaps 10	Autothrottle/autopilot off	2 s	0.5 s
Arm approach	Selecting flaps 10	4 s	1 s
Gear down	Glide-slope intercept/reaching FAF	2 s	0.5 s
Flaps 20	Gear down	2 s	0.5 s
Flaps 25	Reaching 1200 ft	2 s	0.5 s

[a] T = amount of time spent on leg on which the aircraft is 20 nm from field.
[b] T = amount of time spent on leg-before-localizer-intercept heading.
[c] T = amount of time spent on localizer-intercept heading.

next WP will always be met while the speed constraint might not be met (airspeed might be higher than required).

C. Pilot Model and Standard Operating Procedures for the Boeing 747

The pilot manual control model for the FD task consists of a continuous time delay of 0.3 s and a pure gain. All other pilot actions, such as selecting flaps, are modeled according to the SOPs.

Since the aircraft model in the computer simulation is a B747-100, the SOPs that are modeled in the computer simulation are based on the SOPs for a B747: more specifically, the SOPs for the delayed flap approach with flaps land equal to flaps 25. The items of the SOPs that are of importance for the computer simulation are the following (see Fig. 3). Flaps 1 and flaps 5 should be selected before reaching the (localizer) intercept heading. On localizer-intercept heading, the pilot should select flaps 10, arm the approach, and switch to the heading select mode. At glide-slope intercept, the pilot should ask for gear down, flaps 20, and should arm the speedbrake. Finally, at 1200 ft, the pilot is required to select flaps land (equal to flaps 25).

Each of these pilot actions prescribed by the SOPs is modeled using a trigger event (e.g., reaching 1200 ft) and a reaction time representing the time between reaching the trigger event and actually performing the action (e.g., 2 s after reaching 1200 ft, flaps 25 are selected). These reaction times are modeled based on normal distributions. The trigger events and corresponding reaction times as used in the computer simulation are given in Table 1; see also Fig. 4. Since no information could be found regarding the reaction times, the values in Table 1 are a first guess. The trigger events for all actions are explained next.

The SOPs do not give a specified location in the approach where flaps 1 should be selected. Based on conversations with pilots, it was concluded that pilots would select flaps 1 when they are approximately 20 nm (along track) from the field. Therefore, it was decided to use the moment of reaching the starting WP of the leg on which the aircraft is 20 nm from the field (along track) as a trigger event. Based on the same conversations, the trigger event for selecting flaps 5 was chosen to be the moment of reaching the first WP of the leg before localizer-intercept heading (see also Fig. 4).

The first pilot action on localizer-intercept heading modeled in the Monte Carlo simulation is not prescribed by the SOPs, but it follows from the chosen level of automation that is used during the approach (see Fig. 2): this action is autothrottle and autopilot disconnect (for now, assumed to take place simultaneously). The trigger event for this first action on localizer-intercept heading is starting the turn to localizer-intercept heading. The trigger event for the second action on localizer-intercept heading (selecting flaps 10) is the first action on localizer-intercept heading (autothrottle and autopilot disconnect), and so on; see also Fig. 4 and Table 1. The actions on localizer-intercept heading are thus modeled sequentially, always in the same order, although the SOPs do not prescribe a fixed order. Officially, pilots should also switch from LNAV mode to heading select mode on localizer-intercept heading; this switch, however, does not have any impact on the Monte Carlo simulation and is therefore, for now, not modeled. In reality, however, the effect of not switching to heading select mode would cause the pilot considerable difficulty in easily and properly establishing a correct localizer-intercept heading.

Just as for the actions on localizer-intercept heading, the actions gear down and flaps 20 are also always modeled in the same order, although the SOPs do not prescribe this. The trigger event for gear down is glide-slope intercept; however, when the approach is

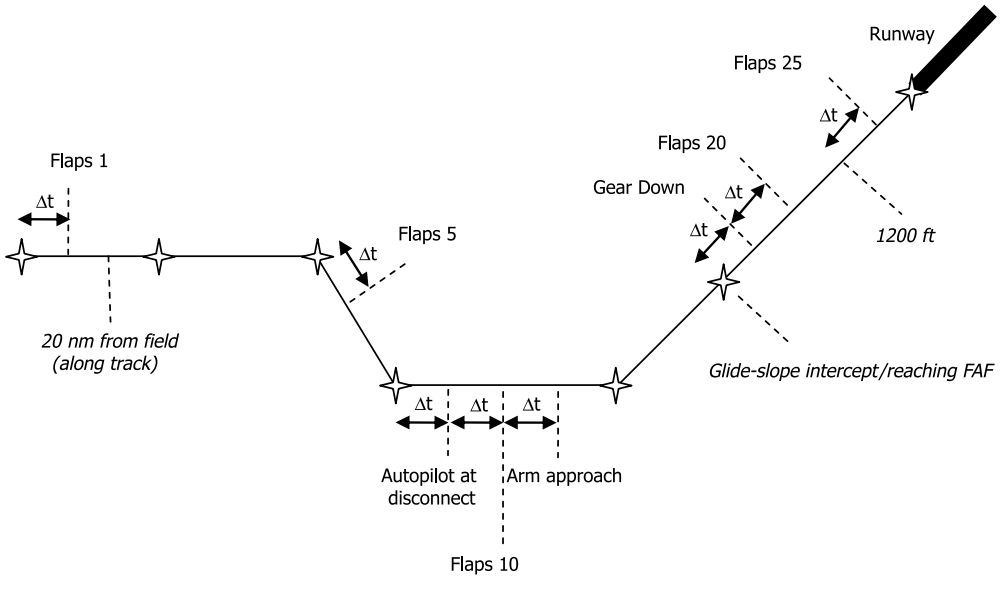

Fig. 4 Visualization of trigger events and reaction times Δt for pilot actions in the Monte Carlo computer simulation.

designed as a continuous descent approach (implying that glide slope could be captured many miles out), the trigger event is reaching the FAF. The trigger event for selecting flaps 20 is the selection of gear down.

The trigger event for selecting flaps 25 (flaps land) is reaching 1200 ft altitude.

It is important to note that, due to simulation technical reasons (for now), only positive reaction times could be modeled in the computer simulation. If any of the distributions for the reaction times in Table 1 yielded a negative number, a new value was created using the same distribution until the value for the reaction times was a positive number. The reaction times are thus based on normal distributions, but they are not necessarily normally distributed. Another important remark concerns the selection of flaps; if the airspeed constraints at the WPs required an airspeed lower than the instantaneous flap speed mark, the next flap setting is selected in the Monte Carlo simulation irrespective of SOPs. For example, if the up mark (speed below which flaps 1 should be selected) is at 220 kt, and the aircraft decelerates to 210 kt because that is the speed constraint at the next WP, then flaps 1 are selected when the airspeed becomes less than 220 kt, even if the aircraft is still 50 nm from the runway.

D. Turbulence and Wind Models

Turbulence is modeled according to the Dryden spectra [15]: the longitudinal scale L_g is fixed in the simulation at 300 m, whereas the turbulence intensity σ is varied according to a Weibull distribution, with $\lambda = 2$ m/s and $k = 2$. The windspeed is modeled using a Weibull distribution ($\lambda = 12.5$ kt and $k = 2.0$). The wind direction is varied around the runway heading by applying a normal distribution with $\mu =$ runway heading and $\sigma = 30°$. During one Monte Carlo simulation run, the turbulence intensity, wind direction, and windspeed are constant throughout the entire approach; between different Monte Carlo runs, these are varied.

E. Outputs of Computer Simulation

The output of the Monte Carlo simulation is a prediction of whether the constraints at the WPs can be met and whether a stabilized approach can be achieved at 1000 ft.

The constraints at a WP were considered to be met when the actual IAS at that WP was less than the required IAS plus 10 kt and the actual altitude at that WP was less than the required altitude plus 100 ft. A lower boundary for these constraints is not necessary, since the Monte Carlo simulation always regulates the airspeed and altitude toward the constraints at the next WP; when the required airspeed and altitude are attained, the Monte Carlo simulation maintains the required airspeed and altitude until the WP is reached. Therefore, in the Monte Carlo simulation, the altitude and airspeed will never be too low at a WP.

To determine whether a Monte Carlo simulation run of the approach resulted in a stabilized approach, the criteria from Sec. II.D were quantified as follows:

1) Heading change and pitch change are within 5°/s.
2) The IAS is not more than VREF plus 20 kt.
3) Flaps 25 are selected, and landing gear is down.
4) The sink rate is not larger than 1000 ft per minute.
5) The localizer and glide slopes are within one dot.

These criteria are evaluated at 1000 ft above airport elevation. An average value is calculated for each of the criteria: for the interval starting 5 s before reaching 1000 ft and ending at 1000 ft. A larger time interval is taken to calculate the average sink rate, since this criterion does not directly refer to the 1000 ft point in itself but refers to the approach. The time interval chosen to calculate the sink rate starts 1 min before reaching 1000 ft, and it ends at 1000 ft. The completion of all checklists and the power setting are, at the moment, not included as criteria for a stabilized approach.

IV. Point Mass Model for Initial Estimates

For rapid evaluation of an approach, a PMM has been developed. This PMM is less accurate but much faster than the nonlinear aircraft model used in the Monte Carlo simulation, and it is used to obtain an initial estimate, whether constraints at the WPs can be met at all and whether a stabilized approach can be achieved. It does so by using the energy rate demand, which is defined as the ratio of the energy rate as commanded by the trajectory $\dot{E}_{\text{cmd}}$ and the minimum energy rate that can be achieved by the aircraft $\dot{E}_{\text{ac}}$. The PMM calculates the energy rate demand for each leg of the approach for a predefined aircraft weight and a predefined windspeed and wind direction. The PMM assumes SOPs, implying that flap and gear settings during the approach are performed according to SOPs.

A. Expression for Energy Rate Demand

The general formula for the energy rate demand is derived next, and the simplifications that result in a formula for the energy rate demand applicable to the PMM are subsequently explained. Additionally, some comments are given on the influence of the aircraft weight on the energy rate demand, since this influence might differ from general perception. The limitations of the predictions of the PMM due to the simplifications that are made are summarized at the end of this section.

Starting with the equation of motion in the direction of flight for an aircraft in a horizontal wind field, and assuming small angles, it is possible to write (see also Fig. 5)

$$\frac{W}{g}\frac{\mathrm{d}}{\mathrm{d}t}(V_a - V_w) = T - D - W\gamma \tag{1}$$

$$\frac{\mathrm{d}x_g}{\mathrm{d}t} = V_a - V_w \tag{2}$$

$$\frac{\mathrm{d}H}{\mathrm{d}t} = V_a\gamma \tag{3}$$

Here, W is the aircraft weight, g is the gravitational acceleration, V_a is the true airspeed in the air path system, V_w is the horizontal windspeed in the geodetic reference frame, V_g is the aircraft speed in the geodetic reference frame, γ is the flight-path angle, T is the aircraft thrust, and D is the aerodynamic drag (see Fig. 5). For the purpose of the PMM, it is necessary to express the energy rate demand in terms of the geodetic reference frame; the kinematic equations (2) and (3) are therefore used:

$$\frac{W}{g}\frac{\mathrm{d}V_a}{\mathrm{d}x_g}(V_a - V_w) - \frac{W}{g}\frac{\mathrm{d}V_w}{\mathrm{d}t} = T - D - \frac{W}{V_a}(V_a - V_w)\frac{\mathrm{d}H}{\mathrm{d}x_g} \tag{4}$$

Assuming a uniform wind field ($V_w = \bar{V}_w =$ constant and $\mathrm{d}V_w/\mathrm{d}t = 0$) and reordering terms yields

$$\frac{W}{g}\frac{\mathrm{d}V_a}{\mathrm{d}x_g}(V_a - V_w) + \frac{W}{V_a}(V_a - V_w)\frac{\mathrm{d}H}{\mathrm{d}x_g} = T - D \tag{5}$$

The energy rate demand can now be expressed in the geodetic reference frame as

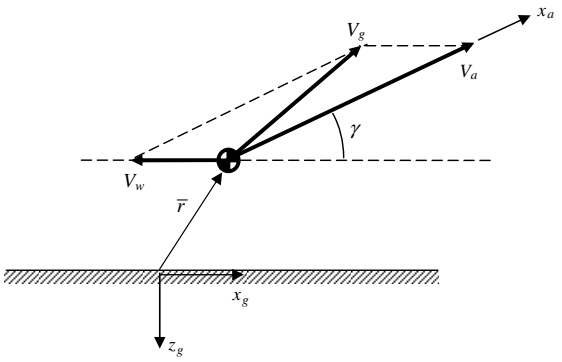

Fig. 5 Definition of air path reference frame and geodetic reference frame.

$$\hat{E} = \frac{[(V_a - V_w)/g](\mathrm{d}V_a/\mathrm{d}x_g) + [(V_a - V_w)/V_a](\mathrm{d}H/\mathrm{d}x_g)}{(T_0/W) - (C_D/C_L)} \quad (6)$$

In this equation, the numerator represents the energy rate as commanded by the trajectory (which will be a negative number in the case of approaches). In the denominator, the value for the flight idle thrust T_0 is used, such that the denominator represents the maximum energy rate (decrease) that can be achieved by the aircraft. Note that, in the case of approaches, this will also be a negative number.

Within the PMM, an average value for airspeed $\bar{V}_a$ and altitude $\bar{H}$ is used for each leg of the approach instead of the instantaneous value; see Fig. 6 for an example. This logically results in an average value for the flight idle thrust $\bar{T}_0$, the aerodynamic drag coefficient $\bar{C}_D$, and the aerodynamic lift coefficient $\bar{C}_L$ for each leg. With this assumption, the expression for the energy rate demand for each leg of the approach [using Eq. (6)] simplifies to

$$\hat{E} = \frac{[(\bar{V}_a - V_w)/g]\Delta V_a + [1 - (V_w/\bar{V}_a)]\Delta H}{[(\bar{T}_0/W) - (\bar{C}_D/\bar{C}_L)]\Delta x_g} \quad (7)$$

This is the expression for the energy rate demand used in the PMM. The PMM also assumes that flaps and gear are selected at the earliest moment possible according to SOPs. For example, flaps 10 should be selected on localizer-intercept heading; therefore, the PMM assumes that flaps 10 are selected at the first WP on localizer-intercept heading (see also Fig. 6). Additionally, the PMM does not consider the flap speed marks; flaps are always selected according to the SOPs.

B. Influence of Aircraft Weight

As stated before, the PMM calculates the energy rate demand for each leg of an approach as a function of, among others, aircraft weight. To understand the predictions of the PMM, it is necessary to understand the influence of aircraft weight on the energy demand ratio. In this light, a common remark heard from pilots is that it becomes more difficult to dissipate energy (and thus to meet the constraints at WPs) with increasing aircraft weight. To verify this remark, Eq. (6) is used.

It can be seen that the rate at which the aircraft can dissipate energy [the denominator in Eqs. (6) and (7)] depends on the ratios of flight idle thrust and weight, the lift coefficient C_L, and the drag coefficient C_D. An increase in weight decreases the flight idle thrust over weight ratio and, in that respect, increases the energy rate demand. Note that the idle thrust is a function of atmospheric pressure, Mach number, ambient temperature, and altitude. However, the aircraft weight also influences the C_D/C_L ratio. When considering a given approach with defined airspeed and altitude constraints, and assuming that the approach is flown according to SOPs, this implies that, at each point of the approach, the airspeed, altitude, flap setting, and gear setting are known and, with this, the values of C_L and C_D for a given aircraft and aircraft weight. When the aircraft weight is increased, the effect on the energy rate demand depends on whether the C_D/C_L ratio decreases or increases (becomes more or less optimal) as a result of this increase in weight for a particular segment of the approach.

For some altitude and airspeed constraints, it is the case that a higher aircraft weight brings about an increase in C_D/C_L ratio larger than the decrease in idle thrust over weight ratio, and it thus diminishes the energy rate demand. For other altitude and airspeed constraints, both ratios will decrease with higher aircraft weight and, as a result, the energy rate demand will increase. This will be illustrated in the case study presented in the next section. It is thus not true that a higher aircraft weight by definition increases the energy rate demand; it depends on the conditions. This is important to keep in mind when analyzing the results of the PMM and Monte Carlo simulation.

C. Reliability of Point Mass Model Predictions

The assumptions made for the PMM influence the reliability of the energy rate demands that are calculated by the PMM. The fact that, during most approaches, flaps and gear will be selected at a later point in time than assumed in the PMM will influence the energy rate demand. Additionally, the assumption of average airspeeds and altitudes has a large effect on the value of the idle thrust and, with that, on the value of the energy rate demand. Comparison of the energy rate demands calculated by the PMM and the energy rate demands that occurred in the Monte Carlo simulation indicated that, in some (extreme) cases, an energy rate demand as high as 1.2 (as predicted by the PMM) would for the same approach result in energy rate demands smaller than one in the Monte Carlo simulation. In other words, the PMM as it is at the moment can give a global indication, which serves well as a first estimate, but it is certainly not accurate. That is also its intended use: when a newly designed approach is analyzed, it will first be analyzed using the PMM for a global indication. Some modifications can then already be made based on these global predictions. After this, a more accurate analysis can be performed using the Monte Carlo computer simulation.

V. Case Study

To demonstrate the predictions of the PMM and the Monte Carlo simulation, the fictitious approach, as illustrated in Fig. 7 (the details of which are summarized in Table 2), is considered. Note that the information as given in Table 2 is the only input required for the Monte Carlo simulation. It can be seen that this is a very short

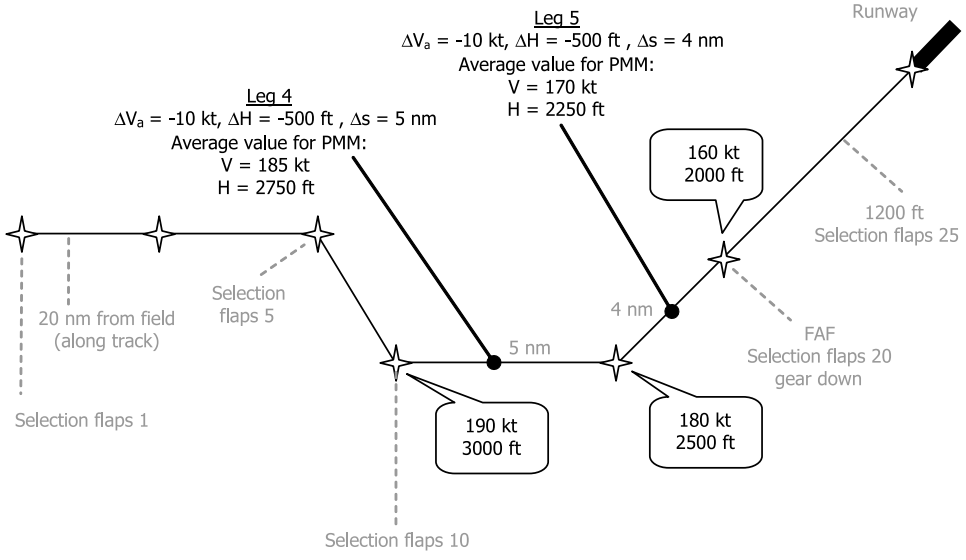

Fig. 6 Example of average values used in the PMM for each leg, and SOPs as assumed in the PMM.

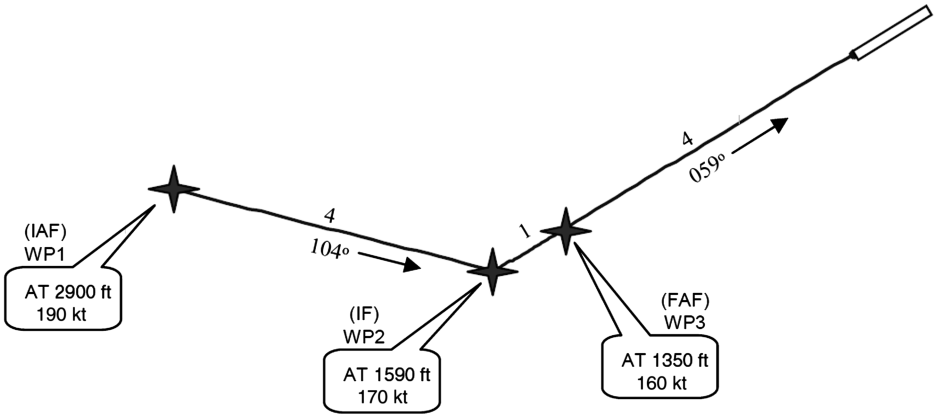

Fig. 7 Approach chart.

continuous descent approach, with a very low FAF at 1350 ft. The only function of the FAF in this case is that pilots are required to select flaps 20 and gear down at the FAF; therefore, this approach with low FAF can also be regarded as a modified procedure for late selection of flaps 20 and gear down. Table 2 shows that the Monte Carlo simulation and PMM will use an IAS equal to VREF plus 5 kt at the threshold. Moreover, the Monte Carlo and PMM simulation will also aim for VREF plus 5 kt at 1000 ft, which is well within the margins for a stabilized approach.

A. Point Mass Model Predictions

To obtain a first indication, this approach is analyzed using the PMM; the results for two different aircraft weights for zero wind conditions are given in Table 3. The PMM assumes that flaps and gear are selected according to SOPs; it does not take into account whether the required speeds are too low for the flap settings prescribed by the SOPs. Table 3 shows that the energy demand ratios (denoted as E ratios in the table) are calculated for five subsequent parts of the approach (note that an E ratio smaller than one indicates that the constraints at the WP can be met); these parts are 1) when flying from WP1 to WP2, energy demand ratios 1.20 and 1.14; 2) when flying from WP2 to WP3, energy demand ratios 1.11 and 1.01; 3) when flying from WP3 to 1200 ft, energy demand ratios 1.27 and 1.20; 4) when flying from 1200 to 1000 ft, energy demand ratios 1.15 and 0.61; and 5) when flying from 1000 ft to the runway, energy demand ratios 0.61 and 0.61.

It can be seen that, for all parts of the approach, the energy demand ratio for the highest aircraft weight (295,000 kg) is lower than the energy demand ratio for the lowest aircraft weight (238,000 kg). This implies that it would be easier to meet the constraints at the WPs and to achieve a stabilized approach (only considering the airspeed) with a higher aircraft weight. For the first three parts of the approach (WP1 to 1200 ft), this is entirely due to the different location on the C_L/C_D curve due to the aircraft weight; see Fig. 8. In Fig. 8, asterisks represent the maximum C_L/C_D value for the lift drag polars, triangles represent C_L/C_D values for the lowest aircraft weight (238,000 kg), and diamonds represent C_L/C_D values for the highest aircraft weight (295,000 kg). It can be seen that for each of these three approach parts, the location of the value of C_L/C_D for the higher aircraft weight is located further away from the maximum (or optimal) C_L/C_D value when compared with the location of the value of C_L/C_D for the lower aircraft weight. This implies that the C_L/C_D value for the higher aircraft weight is smaller than for the lower aircraft weight, which results in a decrease of the energy demand ratio.

Now, for the second to last part of the approach (1200–1000 ft), another factor contributes to the smaller energy demand ratio for the larger aircraft weight than for the lower aircraft weight. The value for VREF for the higher aircraft weight is 161 kt, whereas the value for the lower aircraft weight is 143 kt. This means that, when flying with the higher aircraft weight, it is not necessary to decelerate anymore after reaching WP3 (which has an airspeed constraint equal to 160 kt), whereas when flying with the lower aircraft weight, a deceleration of 12 kt is required to reach the final approach speed equal to VREF plus 5 kt.

Judging from the results of the PMM, it can thus be expected that (for zero wind conditions) it will probably not be possible to achieve a stabilized approach and meet the constraints at the WPs for the lower aircraft weight, since all values for the energy rate demand are (much) larger than one. For the higher aircraft weight, it might be possible to meet the constraints and to achieve a stabilized approach (only considering the airspeed), since the values for the energy rate demand are closer to one. Note that when the PMM would give an exact prediction of the energy rate demand, a value larger than one would mean that the constraints could not be met. However, due to the assumptions in the PMM, a value slightly larger than one could, in reality, still result in meeting the constraints.

Table 2 WPs with altitude and airspeed constraints

WP		Altitude, ft	IAS, kt
WP1	IAF	2900	190
WP2	IF	1590	170
WP3	FAF	1350	160
Runway	——	0	VREF + 5

Table 3 Predictions of the PMM for zero wind conditions and two different aircraft weights

				238,000 kg			295,000 kg		
WP		Flaps	Gear	C_L	C_D	E ratio	C_L	C_D	E ratio
WP1	IAF	10	Up						
WP2	IF	10	Up	0.95	0.071	1.20	1.04	0.079	1.14
WP3	FAF	20	Down	1.13	0.087	1.11	1.24	0.10	1.01
1200 ft		25	Down	1.20	0.12	1.27	1.32	0.14	1.20
1000 ft		25	Down	1.30	0.14	1.15	1.32	0.14	0.61
Runway		25	Down	1.40	0.15	0.61	1.32	0.14	0.61

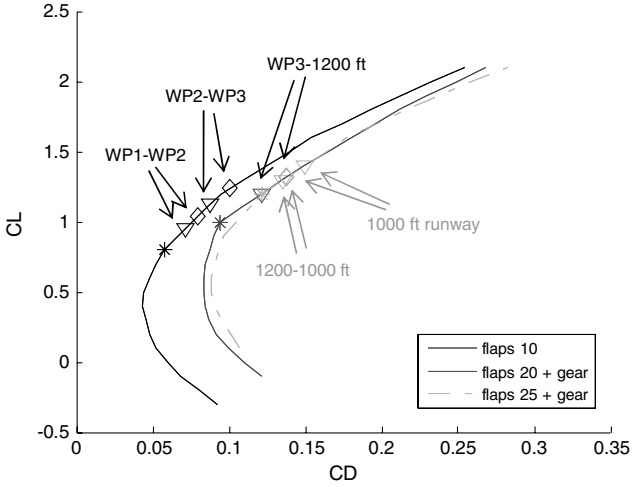

Fig. 8 Lift drag polar for different flap and gear settings.

B. Monte Carlo Simulation Results

The same approach is analyzed using the Monte Carlo simulation. As explained before, the variables within the Monte Carlo simulation are the reaction times for all pilot actions, aircraft weight, wind direction, windspeed, and turbulence intensity. Compared with the PMM, the Monte Carlo simulation uses a more realistic simulation of pilot actions, which also vary in time for each run, and incorporates the effects of varying wind and turbulence.

The trajectory and location of the pilot actions resulting from the Monte Carlo simulation are given for five runs in Fig. 9 for both the low aircraft weight (left) and the high aircraft weight (right). It can be seen that the Monte Carlo simulation stops at 1000 ft; the remainder of the trajectory (until the runway threshold) is indicated in light gray. Since this approach starts at localizer-intercept heading, the Monte Carlo simulation is initialized to start with flaps 5 unless the required airspeed is lower than can be achieved with flaps 5.

For the low aircraft weight, Fig. 9 shows that flaps 10 are indeed selected on localizer-intercept heading, the actions flaps 20 and gear down are performed around the FAF, and flaps 25 are selected at 1200 ft, all according to the SOPs. For the high aircraft weight, however, Fig. 9 indicates that pilot actions will deviate from the SOPs. The airspeed constraints at the WPs are, for the higher aircraft weight, too low to adhere to SOPs. Because of the airspeed constraints, the Monte Carlo will start with flaps 10; additionally, flaps 20 and flaps 25 need to be selected (at 181 and 171 kt, respectively) due to the flap speed marks, which results in the selection of flaps well before the SOPs require them to be selected. The Monte Carlo simulation thus immediately provides the insight that it is impossible to fly this approach according to SOPs with an aircraft weight as high as 295,000 kg.

Whether a stabilized approach was achieved at 1000 ft is depicted in Fig. 10 for 1000 runs with the Monte Carlo simulation. In this figure and the following, a gray circle indicates a stabilized approach was achieved at 1000 ft, and a black dot indicates that the approach was not stabilized at 1000 ft. It should be noted that, in Fig. 10, all unstabilized approaches are due to the fact that the IAS was higher than VREF plus 20 kt; that is, for all approaches, the flap setting, gear setting, localizer deviation, etc. were all according to the criteria given in Sec. III.E when assuming trigger events and reaction times, as defined in Table 1. It can be seen that, for the lower aircraft weight, a stabilized approach can be achieved for windspeeds larger than 10 kt coming from (approximately) runway heading or from a

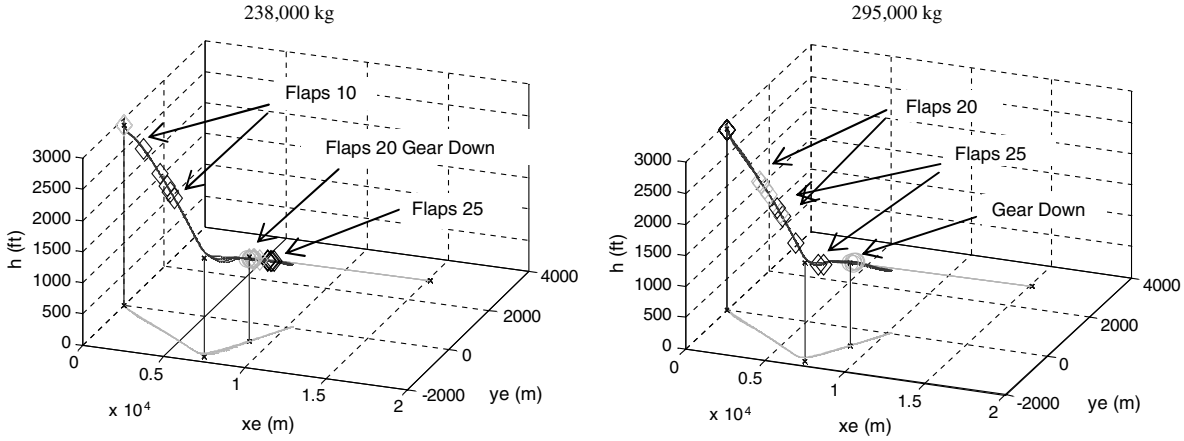

Fig. 9 Trajectory and pilot actions according to Monte Carlo simulation for five runs.

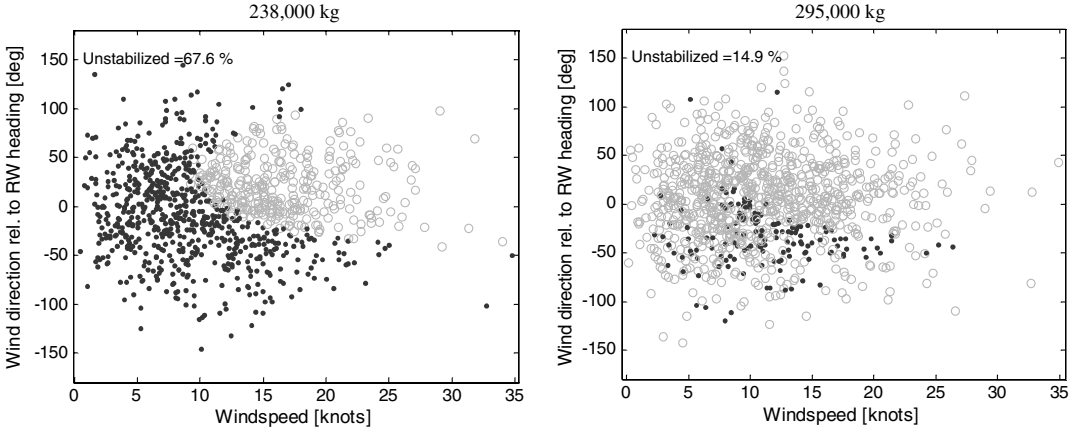

Fig. 10 Results of Monte Carlo simulation ($N = 1000$) for different windspeeds and different wind directions [relative to runway (RW) heading].

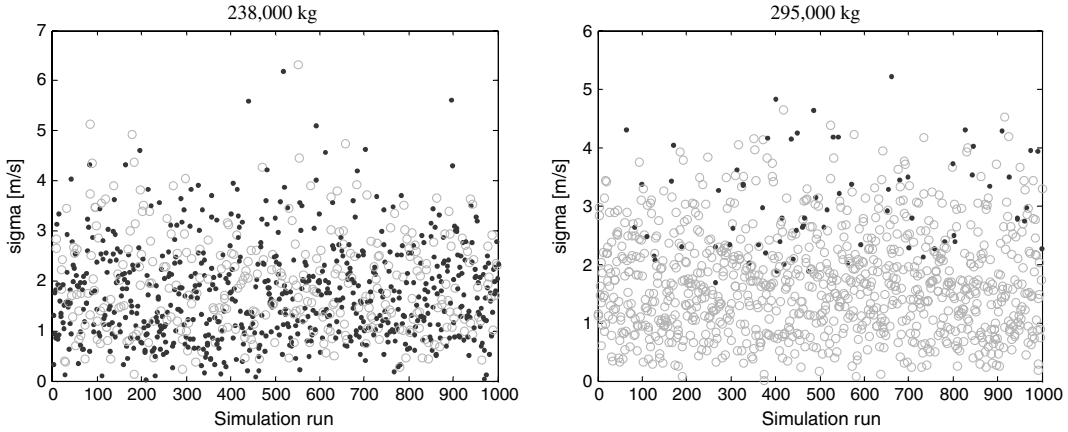

Fig. 11 Turbulence intensity factors σ as used for each run of the Monte Carlo simulation.

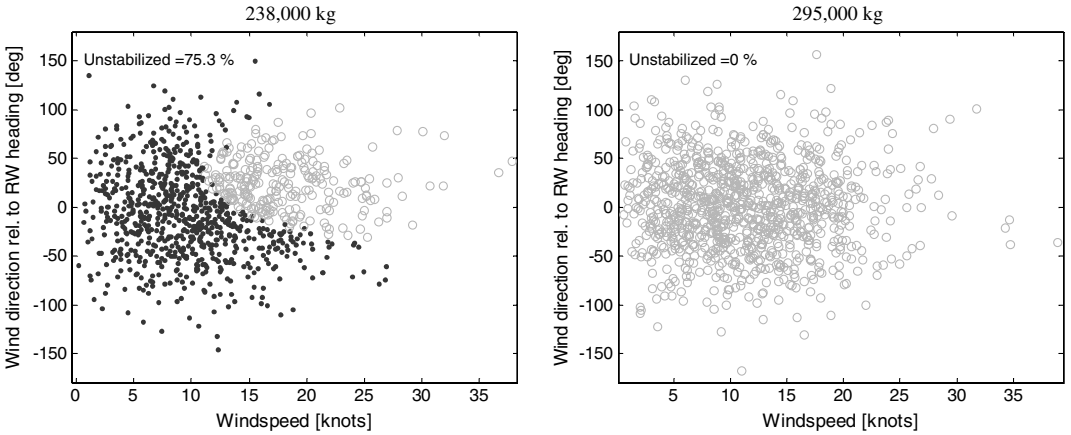

Fig. 12 Results of Monte Carlo simulation ($N = 1000$) for different windspeeds and different wind directions (relative to runway heading), with turbulence intensity factor equal to zero in all runs.

direction slightly larger than runway heading (from the right-hand side of the runway). This makes sense because, in this case, the aircraft would have a considerable headwind on both localizer-intercept heading as well as on final (flying from WP2 to WP3), resulting in more time to meet the constraints and to achieve a stabilized approach.

For the higher aircraft weight, Fig. 10 shows that a stabilized approach can be achieved for all windspeeds and all wind directions. However, in some cases, an unstabilized approach occurs. This is due to the turbulence: when an unfavorable wind direction is combined with a large turbulence gust in the wrong direction, this will result in an unstabilized approach. Figure 11 indeed shows that all unstabilized approaches occur for runs with a very high turbulence intensity factor σ. When running the Monte Carlo simulation again, and using a turbulence intensity factor equal to zero (no turbulence) for all runs, this yields the results given in Fig. 12. Figure 12 indeed demonstrates that all approaches are now stabilized for the higher aircraft weight.

The fact that, for this fictitious approach, more approaches are stabilized for the higher aircraft weight than for the lower aircraft weight is due to the fact that the VREF is higher, due to the fact that flaps 20 and flaps 25 are selected much earlier in the approach (adding more drag to the aircraft for a larger part of the approach) and might, additionally, be due to the smaller energy rate demand as predicted by the PMM. For a stabilized approach, the airspeed at 1000 ft needs to be lower than VREF plus 20 kt. This implies that the airspeed should be lower than 181 kt for the high aircraft weight and lower than 163 kt for the low aircraft weight. The aircraft with the higher weight thus needs to decelerate less in the last part of the approach than the aircraft with the lower weight. This effect is entirely due to the different numerical values that result from the airspeed criterion for a stabilized approach; it has, in itself, nothing to do with the ability of the aircraft to dissipate energy.

The Monte Carlo simulation also calculates whether the constraints at the WPs are met. As an example, Table 4 gives an overview of the percentage of flights during which the constraints were met at WP2, for flights with turbulence, and flights without turbulence ($\sigma = 0$ m/s). It can be seen that, for the higher aircraft weight, a higher percentage of flights meets the constraints at the WP. The fact that the constraints are not met is always due to the fact that the airspeed is too high. The VNAV mode will direct the aircraft toward the required altitude and, second to this, the autothrottle controls the airspeed. When the path is too steep (i.e., the energy rate demand is too high), the autothrottle cannot regulate the airspeed toward the desired value, even when applying idle thrust. In reality, when this occurs, a drag required message appears (see also the accompanying paper [4]), and pilots will use speedbrakes in an attempt to meet the constraints. However, within this flight mechanical assessment tool that is to be used during the design of

Table 4 Percentage of approaches during which the constraints at WP2 were met according to the Monte Carlo simulation ($N = 1000$); results given for simulations with turbulence and without turbulence ($\sigma = 0$)

	WP2, %
238,000 kg	11.4
295,000 kg	90.9
238,000 kg, $\sigma = 0$ m/s	10.7
295,000 kg, $\sigma = 0$ m/s	93.5

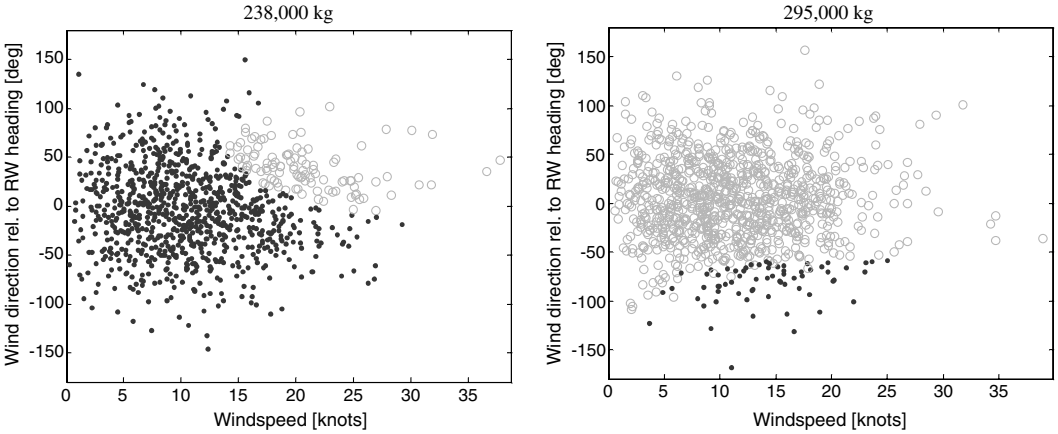

Fig. 13 Results of Monte Carlo simulation ($N = 1000$) for WP2, for different windspeeds and different wind directions (relative to runway heading).

approaches, speedbrakes are not incorporated, since the premise is that approaches should be designed such that they can be flown without the use of speedbrakes.

The results for WP2 are visualized as a function of windspeed and wind direction in Fig. 13. A gray circle indicates the altitude and airspeed constraints were met at WP2, and a black dot indicates that the constraints were not met at WP2. Figure 13 shows that, for the lower aircraft weight, the constraints at WP2 are not met unless there is a considerable headwind when flying from WP1 to WP2. For the higher aircraft weight, the constraints at WP2 are met unless the aircraft experiences a tailwind while flying from WP1 to WP2.

In conclusion, it can be stated that for this particular approach with these airspeed and altitude constraints, the aircraft with the higher weight performs better than the aircraft with the lower weight. The fact that the higher aircraft weight shows better results, however, is not necessarily true for other approaches as well. It depends on the combination of three factors, which can combine into better or worse performance. The three factors are 1) the value of the energy rate demand for the particular aircraft weight, 2) the value of the VREF for the particular aircraft weight (which determines how much the aircraft needs to decelerate in the last part of the approach), and 3) whether or not the approach can be flown according to SOPs for that aircraft weight. (With increasing aircraft weight, the chance increases that flaps need to be selected before the SOPs require them to be selected. This in itself is not desirable since, the approach can, in this case, not be flown according to SOPs; however, it will result in better deceleration characteristics due to the additional drag caused by the flaps.)

C. Regression

A stepwise linear regression analysis was performed for this particular approach on the results of the Monte Carlo simulation in order to determine which variables modeled in the Monte Carlo simulation have an influence on whether the constraints at the WPs can be met and whether or not a stabilized approach was achieved at 1000 ft.

The first regression presented in this section concerns the stabilized (or unstabilized) approaches at 1000 ft. Since the only reason for the unstabilized approaches in the Monte Carlo simulation was the fact that the IAS was higher than VREF plus 20 kt at 1000 ft, a prediction of whether the approach is stabilized can be directly derived from a prediction of the IAS at 1000 ft. Therefore, the IAS at 1000 ft is chosen as dependent measure for the regression analysis. A regression is performed for the two aircraft weights separately, as well as for the results of the two aircraft weights combined; see Table 5. The predictors for the regression are the inputs for the Monte Carlo simulation, and they are listed vertically in the first column of Table 5. The entries show the value of R^2, the number in parentheses indicates the step at which the predictor was added to the regression. The maximum difference between R^2 and adjusted R^2 values in this table is 0.2%. No multicollinearity can be assumed: for all predictors, the variance inflation factor (VIF) is smaller than 1.8 (and hence the tolerance is larger than 0.55).

It can be seen that the R^2 value for the lower aircraft weight (0.951) is substantially larger than the R^2 value for the higher aircraft weight (0.138). This can be explained by the fact that, for the higher aircraft weight, more approaches are stabilized; therefore, a large percentage of the approaches will achieve an IAS equal to VREF plus 5 kt at 1000 ft, independent of the value of the predictor variables. As a result, there will be less correlation between the IAS at 1000 ft (largely constant between many runs) and the predictors. This effect can also be seen in the results of the regression for both aircraft weights.

Therefore, in the authors' opinions, the regression model for the lower aircraft weight gives the best indication of predictors that influence the IAS at 1000 ft, and thus the predictors that influence the chance of achieving a stabilized approach (first column in Table 5). This regression model is given in Table 6. It can be seen that the wind direction (represented by the predictor headwind on final and the headwind on localizer-intercept heading) has the largest influence on the IAS at 1000 ft, which agrees with the discussion of the Monte Carlo simulation results shown in Fig. 12. Additionally, the reaction time in pilot actions for the actions flaps 20, flaps 25, and gear down also influence the IAS at 1000 ft but to a much lesser extent. However, for these pilot reaction times, one would expect positive standardized β values, since a larger reaction time represents a delay in adding more drag to the aircraft and is thus expected to result in a higher IAS at 1000 ft. This is not the case for the standardized β value for the flaps 20 reaction time; therefore, it is better to use the regression model given in step 4 (Table 6) or even use the regression model given in step 2 since, with only two predictors, an R^2 value of 0.948 is already achieved. For this particular approach,

Table 5 Results of a stepwise linear regression for dependent measure IAS at 1000 ft (probability of F to enter ≤ 0.05; probability of F to remove ≥ 0.01)[a]

	238,000 kg, $\sigma = 0$	295,000 kg, $\sigma = 0$	Both masses, $\sigma = 0$
Flaps 10 reaction time	——	——	——
Approach arm reaction time	——	——	——
Autopilot flight director switch reaction time	——	0.138 (3)	0.623 (5)
Flaps 20 reaction time	0..951 (5)	——	——
Gear down reaction time	0..949 (3)	——	0..622 (4)
Flaps 25 reaction time	0.951 (4)	——	——
Headwind on final	0..948 (2)	0..135 (2)	0..621 (3)
Headwind on localizer-intercept heading	0..915 (1)	0..049 (1)	0..616 (2)
σ	N/A	N/A	N/A
Aircraft mass	N/A	N/A	0.479 (1)

[a]Predictors listed vertically.

Table 6 Stepwise linear regression model for dependent measure IAS at 1000 ft, aircraft mass 238,000 kg, without turbulence

	B	Standard error B	β	R^2	Adjusted R^2
Step 1					
Constant, kt	167.53	0.043			
Headwind on localizer-intercept heading, kt	−4.78	0.005	−0.957 [a]	0.915	0.915
Step 2					
Constant, kt	168.22	0.044			
Headwind on localizer-intercept heading, kt	−0.402	0.005	−0.803 [a]		
Headwind on final, kt	−0.136	0.005	−0.237 [a]	0.948	0.947
Step 3					
Constant, kt	167.798	0.083			
Headwind on localizer-intercept heading, kt	−0.401	0.005	−0.802 [a]		
Headwind on final, kt	−0.137	0.005	−0.237 [a]		
Gear down reaction time, s	0.210	0.035	0.042 [a]	0.949	0.949
Step 4					
Constant, kt	137.43	0.109			
Headwind on localizer-intercept heading, kt	−0.401	0.005	−0.802 [a]		
Headwind on final, kt	−0.136	0.005	−0.236 [a]		
Gear down reaction time, s	0.210	0.035	0.042 [a]		
Flaps 25 reaction time, s	0.182	0.035	0.037 [a]	0.951	0.950
Step 5					
Constant, kt	167.61	0.131			
Headwind on localizer-intercept heading, kt	−0.402	0.005	−0.803 [a]		
Headwind on final, kt	−0.136	0.005	−0.236 [a]		
Gear down reaction time, s	0.208	0.035	0.042 [a]		
Flaps 25 reaction time, s	0.181	0.035	0.037 [a]		
Flaps 20 reaction time, s	0.088	0.035	−0.018 [b]	0.951	0.951

[a] $p < 0.001$.
[b] $p = 0.012$.

pilot actions that occur earlier in the approach, such as selecting flaps 10, do not appear to influence the IAS at 1000 ft.

The second linear stepwise regression is performed for meeting the constraints at WP2. As explained before, the altitude constraints are always met, so the reason for not meeting the constraints is an airspeed that is too high. Therefore, the dependent measure is chosen to be the IAS at WP2. Table 7 shows that the R^2 value is again considerably lower for the higher aircraft weight than for the lower aircraft weight; this is because of the same reasons as given previously (for the higher aircraft weight, a large percentage of the flights did meet the constraints; therefore, a large percentage of the flights arrived at and remained at 170 kt). Therefore, the regression model for the lower aircraft weight is again considered; it is given in Table 8. It can be seen that the amount of headwind on localizer-intercept heading is by far the most important predictor. This agrees with the results shown in Fig. 13 and the discussion of the results of the Monte Carlo simulation.

D. Comparison of Results

The results of the Monte Carlo simulation seem credible and can be explained when considering the influence of windspeed, wind direction, and turbulence on meeting the constraints at WPs and achieving a stabilized approach at 1000 ft. This is true for both aircraft weights.

Table 7 Results of a stepwise linear regression for the dependent measure IAS at WP2. The predictors are listed vertically. The maximum difference between R^2 and adjusted R^2 values is 1.5%. The VIF is smaller than 1.1

	238,000 kg$\sigma = 0$	295,000 kg$\sigma = 0$	Both masses$\sigma = 0$
Flaps 10 reaction time	——	——	——
Approach arm reaction time	0.946 (2)	——	——
Autopilot flight director switch reaction time	——	0.426 (2)	0.882 (3)
Headwind on localizer-intercept heading	0.946 (1)	0.421 (1)	0.881 (2)
σ	N/A	N/A	N/A
Aircraft mass	N/A	N/A	0.673 (1)

Table 8 Stepwise linear regression model for the dependent measure IAS at WP2, aircraft mass 238,000 kg, without turbulence

	B	Standard error B	β	R^2	Adjusted R^2
Step 1					
Constant, kt	186.66	0.032			
Headwind on localizer-intercept heading, kt	−0.451	0.003	−0.973 [a]	0.946	0.946
Step 2					
Constant, kt	186.46	0.100			
Headwind on localizer-intercept heading, kt	−0.451	0.003	−0.973 [a]	0.946	0.946
Approach arm delay	0.049	0.024	0.015 [b]	0.946	0.946

[a] $p < 0.001$.
[b] $p = 0.04$.

The results of the regression analysis correspond very well with the explanation of the results of the Monte Carlo simulation for the lower aircraft weight. The regression analysis indicated that the windspeed and wind direction had the largest influence on meeting the constraints at WPs and achieving a stabilized approach at 1000 ft, whereas the pilot reaction times for selecting flaps and gear according to SOPs did not have a large influence or had no influence at all. This can, however, be due to the fact that the reaction times for all pilot actions in the Monte Carlo simulation (see Table 1) were chosen too small.

For the higher aircraft weight, the regression analysis did not yield good results in terms of R^2, and it did not correspond with the explanation of the results of the Monte Carlo simulation. This is because, for the higher aircraft weight, most of the time, the constraints could be met, and a stabilized approach was achieved, resulting in a constant value for the dependent measure (IAS) for a very large percentage of all approaches, which logically influenced the regression analysis.

The predictions of the PMM approximately agreed with the results of the Monte Carlo simulation for the lower aircraft weight, since for this weight, the approach could indeed be performed according to SOPs. If the airspeeds required by the approach were too low (i.e., when due to the required airspeed flaps needed to be selected earlier in the approach than prescribed by SOPs), the predictions of the PMM were based on an unrealistic flap schedule (strictly adhering to the SOPs in Figs. 3 and 4) and therefore did not correspond to the results of the Monte Carlo simulation. This was the case for the higher aircraft weight.

VI. Conclusions

A flight mechanical assessment tool based on a Monte Carlo simulation was presented that predicts, given the aircraft, the SOPs, the wind conditions, and the approach trajectory, the percentage of flights that will not meet the constraints at the WPs and will not achieve a stabilized approach. These two factors affect, among others, pilot TDL during approach [4]. The flight mechanical assessment tool is intended to be used during the design of approaches.

The predictions of the Monte Carlo simulation seem plausible. The predictions were analyzed by visually inspecting the plots with results and by regression analyses. For the approach considered in the case study, the dominating factors influencing whether the constraints at WPs could be met and whether a stabilized approach could be achieved were the windspeed, wind direction, and aircraft weight. The moments in time at which the pilots performed all their actions (such as selecting gear or flaps) appeared to have only a very small influence or no influence at all. This could, however, be due to the assumptions that were made regarding these moments in time where the actions are performed; it could be that these were chosen too optimistically.

The predictions of the Monte Carlo simulation, as well as the modeling of pilot actions within the Monte Carlo simulation, have to be validated by flight simulator tests. This is done in the accompanying paper [4]. The paper will show that reliable predictions by the Monte Carlo simulation can indeed be obtained by modeling pilot actions according to SOPs and applying a distribution in time for all these actions. This conclusion is based on the comparison of the predictions of the Monte Carlo simulation to the data from the flight simulator tests. However, the accompanying paper [4] will also demonstrate that better results can be obtained when some of the trigger events, as assumed in this paper, are replaced by different trigger events. For example, in the current paper, the selection of flaps 1 was based on the trigger event reaching 20 nm from field, whereas the results of the flight simulator data showed that reaching a certain IAS was a better trigger event. Additionally, the flight simulator test results in the accompanying paper [4] will demonstrate that the distribution of the reaction times for most pilot actions were more widely spread than assumed in the current paper.

The PMM presented in this paper will need to be refined because, as it is, its predictions are not accurate enough to be used confidently during the design of approaches. The goal is to use the Monte Carlo simulation and flight simulator tests to identify the factors that have an influence on whether the constraints can be met and a stabilized approach can be achieved, and to incorporate these factors in detail in the PMM. This refined PMM is expected to yield more reliable results.

Acknowledgment

This research was financially supported by the Dutch Technology Foundation STW (DLR7071).

References

[1] "Killers in Aviation: FSF Task Force Presents Facts About Approach-and-Landing and Controlled-Flight-Into-Terrain Accidents," *Flight Safety Digest*, Nov. 1998–Feb. 1999, pp. 1–278.

[2] *Statistical Summary of Commercial Jet Airplane Accidents, Worldwide Operations: 1959–2005*, Boeing Commercial Airplane Group, Seattle, WA, May 2006, pp. 1–26.

[3] *Navigation Strategy for ECAC*, Edition 2.1, EUROCONTROL: European Organisation for the Safety of Air Navigation, Belgium, 15 March 1999.

[4] Heiligers, M. M., Van Holten, T., and Mulder, M, "Factors That Influence Pilot Task Demand Load During Area Navigation Approaches," *Journal of Aircraft*, Vol. 48, No. 3, 2011, pp. 975–994.

[5] Stassen, H. G., Johannsen, G., and Moray, N., "Internal Representation, Internal Model, Human Performance Model and Mental Workload," *Automatica*, Vol. 26, No. 4, 1990, pp. 811–820. doi:10.1016/0005-1098(90)90057-O

[6] Godley, S. T., "Perceived Pilot Workload and Perceived Safety of RNAV (GNSS) Approaches," Australian Transport Safety Bureau Rept. 20050342, Canberra, Australia, 2006.

[7] Heiligers, M. M., Van Holten, T., and Mulder, M., "Predicting Pilot Task Demand Load During Final Approach," *International Journal of Aviation Psychology*, Vol. 19, No. 4, Oct.–Dec. 2009, pp. 391–416. doi:10.1080/10508410902983987

[8] Baron, S., Zacharias, G., Muralidharan, R., and Lancraft, R., "PROCRU: A Model for Analyzing Flight Crew Procedures in Approach to Landing," *NASA-MIT 16th Annual Manual 1980*, 1980, pp. 488–520.

[9] Baron, S., Kruser, D. S., and Huey, M. B., *Quantitative Modeling of Human Performance in Complex, Dynamic Systems*, National Academy Press, Washington D.C., 1990, pp. 1–108.

[10] Corker, K. M., "Human Performance Simulation in the Analysis of Advanced Air Traffic Management," *Proceedings of the 1999 Winter Simulation Conference*, edited by P. A. Farrington, H. B. Nembhard, D. T. Sturrock, and G. W. Evans, Vol. 1, 1999, pp. 821–828.

[11] Gore, B. F., and Corker, K. M., "A Systems Engineering Approach to Behavioral Predictions of an Advanced Air Traffic Management Concept," *19th Digital Avionics Systems Conference, Entering the Second Generation of Powered Flight*, Philadelphia, 2000, pp. 4B3/1–4B3/8.

[12] Smith, B. R., and Tyler, S. W., "The Design and Application of MIDAS: A Constructive Simulation for Human-System Analysis," *2nd Simulation Technology and Training Conference*, Canberra, Australia, 1997.

[13] Vicente, K. J., *Cognitive Work Analysis, Towards Safe, Productive, and Healthy Computer-Based Word*, Lawrence Erlbaum Assoc., Mahwah, NJ, 1999, pp. 1–416.

[14] Hanke, R. C., and Nordwall, D. R., "The Simulation of a Jumbo Jet Transport Aircraft Volume II: Modeling Data," NASA Rept. D6-30643, Sept. 1970, pp. 1–647.

[15] Etkin, B., *Dynamics of Atmospheric Flight*, Wiley, New York, 1972, pp. 1–580.